δ 1.24 (m, 6 H, 2-H, 6-H, 7-H), 1.51 (m, 7 H, 3-H, 4-H, 5-H, 8-H), 1.51 (s, 6 H, 2'-H, 4'-H, 5'-H), 2.39 (s, 1 H, 3'-H); ^{13}C NMR δ 24.1 (C-4), 25.6 (C-3'), 25.8 (C-3, C-5, C-8), 27.0 (C-2, C-6, C-7), 29.2 (C-1), 46.4 (C-2', C-4', C-5'), 52.0 (C-1'); IR (CCl_4 or CS_2) 2960, 2931, 2903, 2858, 1294, 1197, 1133 cm^{-1}; MS *m/z* (relative intensity) 175 (1), 161 (5), 147 (33), 133 (14), 119 (31), 105 (68), 91 (100), 79 (85), 77 (38), 67 (68), 55 (31), 53 (27).

1,4-Bis(bicyclo[1.1.1]pent-1-yl)bicyclo[2.2.2]octane (9b). The mixture of **7a** and **9a** with **7a** as a major product yielded 9 mg of **9b** (62%, based on 0.06 mmol of **5**): mp 204-206 °C; ^{1}H NMR δ 1.24 (s, 12 H, 2-H, 3-H, 5-H, 6-H, 7-H, 8-H), 1.51 (s, 12 H, 2'-H, 2''-H, 4'-H, 4''-H, 5'-H, 5''-H), 2.39 (s, 2 H, 3'-H, 3''-H); ^{13}C NMR δ 25.7 (C-3', C-3''), 27.2 (C-2, C-3, C-5, C-6, C-7, C-8), 29.8 (C-1, C-4), 46.5 (C-2', C-2'', C-4', C-4'', C-5', C-5''), 51.8 (C-1', C-1''); IR (CCl_4 or CS_2) 2962, 2934, 2907, 2869, 1309, 1200, 1134, 1047, 920 cm^{-1}; MS *m/z* (relative intensity) 213 (1), 201 (1), 185 (2), 173 (5), 159 (7), 145 (18), 131 (24), 119 (34), 105 (53), 91 (100), 79 (73), 67 (48), 53 (30).

Acknowledgment. This research was supported by the National Science Foundation (Grant CHE 8796257), the Texas Advanced Research Program, and the Welch Foundation. K.H. is grateful to the Alexander von Humboldt Foundation for a Feodor Lynen fellowship. We are obliged to Dr. J. Kopecký for a kind gift of 1,4-diiodobicyclo[2.2.2]octane.

Registry No. 1, 35634-10-7; **4**, 97229-08-8; **5**, 10364-05-3; **6a**, 124381-06-2; **6b**, 124381-10-8; **7a**, 124381-07-3; **7b**, 124381-11-9; **8a**, 124381-08-4; **8b**, 124381-12-0; **9a**, 124381-09-5; **9b**, 124381-13-1.

Supplementary Material Available: Full details of the X-ray experiment, atomic positional and thermal parameters, bond lengths and angles, and a thermal ellipsoid plot showing the atom labeling scheme (10 pages); a listing of observed and calculated structure factor amplitudes (11 pages). Ordering information is given on any current masthead page.

Nucleophilic Substitution at Oxygen: The Reaction of PH_3 and NH_3 with H_3NO. An ab Initio Investigation

Steven M. Bachrach

Northern Illinois University, Department of Chemistry, DeKalb, Illinois 60115

Received April 3, 1989 (Revised Manuscript Received September 18, 1989)

The oxygen transfer reaction between H_3NO and NH_3 or PH_3 is examined using ab initio calculations. The identity reaction involving H_3NO and NH_3 is calculated to have a barrier of 30.39 kcal mol^{-1} at HF/6-316*. This barrier increases to 37.34 kcal mol^{-1} with the inclusion of electron correlation through MP2. The N-O-N angle in the transition state is 180°, confirming a classical backside attack. The energy of reaction of H_3NO with PH_3 is calculated to be -65.5 kcal mol^{-1} with a barrier height of 30.5 kcal mol^{-1} at HF/6-31+G*//HF/6-31G*. The N-O-P angle in the transition state is 170.5°, suggesting that the reaction proceeds via the S_N2 mechanism. An early transition state is indicated by the reaction energetics and bond lengths. No stable intermediate was found for either reaction, confirming a single-step mechanism.

Geometric requirements of nucleophilic displacement reactions can be evaluated using systems which have the reacting centers tied together by a few intervening atoms. This linkage provides a cyclic transition state (TS) which imposes distinct restrictions upon the bond angles at the reacting center. Eschenmoser's classic experiments on the S_N2 reaction at carbon clearly established the requirement of a near linear arrangement of the nucleophile, carbon, and leaving group.[1] Similar studies have examined ring formation,[2] nucleophilic substitution at sulfur,[3] and displacement reactions at anionic nitrogen.[4] Beak and Loo recently examined displacement reactions at oxygen.[5] Their findings of first-order kinetics in reaction 1 suggest

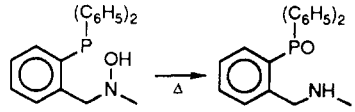

(1)

that this reaction does not proceed by the classic S_N2 mechanism. A linear arrangement of nucleophile and leaving group necessitates an intermolecular reaction and second-order kinetics for reaction 1. To further understand the mechanism of displacements at heteroatoms, we report ab initio calculations for a related reaction, reaction 2, which differs from reaction 1 by employing an *N*-oxide rather than a hydroxylamine. Reaction 2 is acyclic, but knowledge of the TS geometry in this reaction will indicate whether a cyclic intramolecular reaction is possible. We also examine the identity reaction between ammonia and ammonia oxide, reaction 3, to compare any difference between nitrogen and phosphorus as nucleophilic agents toward oxygen.

$$NH_3O + PH_3 \rightarrow NH_3 + PH_3O \quad (2)$$

$$NH_3O + NH_3 \rightarrow NH_3 + NH_3O \quad (3)$$

Computational Methods

All calculations were performed at the Hartree-Fock (HF) self-consistent field level using GAUSSIAN-86.[6] All structures were fully optimized within the constraints of the appropriate point group using the 3-21G,[7a] 3-21G(*),[6]

(1) Tenud, L.; Farooq, S.; Seible, J.; Eschenmoser, A. *Helv. Chim. Acta* **1970**, *53*, 2059.
(2) Baldwin, J. E.; Lusch, M. J. *Tetrahedron* **1982**, *38*, 2939.
(3) Andersen, K. K.; Malver, O. *J. Org. Chem.* **1983**, *48*, 4803.
(4) Beak, P.; Basha, A.; Kokko, B. *J. Am. Chem. Soc.* **1984**, *106*, 1511.
(5) Beak, P.; Loo, D. *J. Am. Chem. Soc.* **1986**, *108*, 3834.
(6) Frisch, M.; Binkley, J. S.; Schlegel, H. B.; Raghavachari, K.; Martin, R.; Stewart, J. J. P.; Bobrowicz, F.; DeFrees, D.; Seeger, R.; Whiteside, R.; Fox, D.; Fluder, E.; Pople, J. A. GAUSSIAN-86, Release C, Carnegie-Mellon University.
(7) (a) Binkley, J. S.; Pople, J. A.; Hehre, W. J. *J. Am. Chem. Soc.* **1980**, *102*, 939. (b) Francl, M. M.; Pietro, W. J.; Hehre, W. J.; Binkley, J. S.; Gordon, M. S.; DeFrees, D. J.; Pople, J. A. *J. Chem. Phys.* **1982**, *77*, 3654.

0022-3263/90/1955-1016$02.50/0

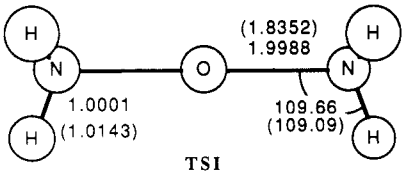

TSI

Figure 1. Geometry of the calculated transition structure for reaction 3, TSI. Results are listed for the HF/6-31G* TS with MP2/6-31G* results in parentheses. All distances are in angstroms and all angles are in degrees.

and 6-31G*[7b] basis sets. The nature of each optimized structure was determined using analytical frequencies. Minimum-energy structures had no imaginary frequencies, and all transition structures had one imaginary frequency. The frequencies were used to obtain zero-point vibrational energies, which have been scaled by 0.89 to correct for their inherent overestimation at this computational level.[8] Topological electron density analysis was performed using EXTREME.[9]

Results

We investigated two possible pathways for the reaction. The first merchanism involved a stable intermediate of the form H_3N–O–NH_3 or NH_3–O–PH_3. Despite an extensive search of the potential surfaces, no stable intermediate for either reaction was located. For the former case, optimization led to the transition structure described below. Optimization toward a stable NH_3–O–PH_3 intermediate lead instead to dissociation of the two fragments. We then turned our efforts toward locating a transition state corresponding to a one-step reaction.

The transition structure for the identity reaction given in reaction 3 was optimized under D_{3h} symmetry using the 3-21G and 6-31G* basis sets. The geometry of the 6-31G* transition structure (TSI) is shown in Figure 1. For both cases, this highly symmetrical structure was found to have only one imaginary vibrational frequency.

The energy barrier for reaction 3 is 13.00 kcal mol^{-1} at 3-21G. This barrier is increased to 30.39 kcal mol^{-1} at 6-31G*. The zero-point energy difference between reactants and transition structure is less than 0.5 kcal mol^{-1}, and, consequently, we will neglect it. We were concerned about the effects of correlation on the reaction barrier. Consequently, we optimized the structures of NH_3 and $H_3N{=}O$ at MP2/6-31G*. The transition structure was also optimized at this level, again maintaining D_{3h} symmetry. The MP2 transition structure has a shorter N–O distance (1.835 Å) than in the HF/6-31G* transition structure (1.989 Å). The energy barrier at the MP2 level is 37.34 kcal mol^{-1}, indicating that while correlation is certainly important in determining accurate reaction energetics, basic trends and concepts can be deduced with calculations employing polarized basis sets at the HF level.

To determine the course of reaction 2, we first optimized the geometry of the PH_3–O–NH_3 transition structure using the 3-21G basis set and restricting the N–O–P angle to 180°, resulting in TS1. This structure has one imaginary frequency and is a transition state. However, optimization of TS1 (i.e. the N–O–P angle restricted to 180°) using the 3-21G(*) basis set, which adds d-functions to phosphorus, gave a structure having three imaginary frequencies and is therefore not a transition state (TS).

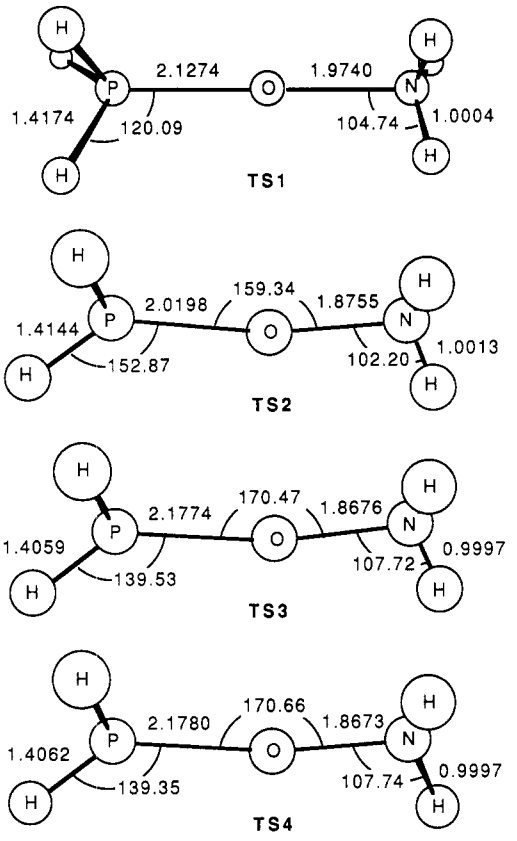

Figure 2. Geometries of calculated transition states for reaction 2. All distances are in angstroms and all angles in degrees.

Table I. Relative Energies (kcal mol^{-1}) of the Components of Reaction 2

basis set	$NH_3O + PH_3$	TS	$NH_3 + PH_3O$
3-21G//3-21G	22.23	39.60	0.0
3-21G(*)//3-21G(*)	68.37	81.25	0.0
6-31G*//6-31G*	68.60	96.91	0.0
6-31+G*//6-31G*	65.53	95.85[a]	0.0

[a] Calculated at the geometry of TS3.

Optimization allowing the P–O–N angle to vary then yielded TS2, which has one imaginary frequency. The N–O–P angle is 159.34°. Starting with TS2, reoptimization using the larger 6-31G* basis set (d-functions on all heavy atoms) gave TS3. The N–O–P angle is 170.47°, more than 11° larger than the corresponding angle in TS2. TS3 has two imaginary frequencies and is not a TS. However, the second frequency is very small (9.95i cm^{-1}), so the true TS will not be significantly lower in energy.

Finally, we ran the geometry optimization with the 6-31G* basis set with no symmetry restrictions, giving TS4. This structure indeed had only one imaginary frequency and is the actual TS. TS4 is nearly of C_s symmetry; the NH_3 group is rotated about 1° from the symmetry plane. TS4 lies 1 microhartree in energy below TS3, with the lowest positive frequency (only 13.4 cm^{-1}) corresponding to NH_3 rotation. The geometric parameters of these structures are shown in Figure 2.

The N–O–P angle in TS4 is 170.66°, clearly a bent structure in contrast to the linear transition structure for reaction 3. The N–O and P–O bond lengths are 1.867 and 2.178 Å, respectively. The corresponding bond lengths in H_3NO and H_3PO are 1.376 and 1.464 Å. Based on the difference in the changes of the P–O and N–O distances, the formation and breakage of the N–O and P–O bonds are not symmetrical in the TS.

(8) Hehre, W. J.; Radom, L.; Schleyer, P. v. R.; Pople, J. A. *Ab Initio Molecular Orbital Theory*; J. Wiley and Sons: New York, 1986.
(9) Biegler-Konig, F. W.; Bader, R. F. W.; Tang, T. H. *J. Comput. Chem.* **1982**, *3*, 317. We thank Prof. R. F. W. Bader and P. MacDougall for a VAX copy of this program.
(10) Chandrasekhar, J.; Andrade, J. G.; Schleyer, P. v. R. *J. Am. Chem. Soc.* **1981**, *103*, 5609.

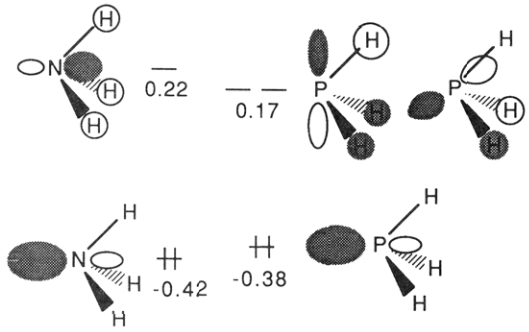

Figure 3. Frontier molecular orbitals of ammonia and phosphine. Orbital energies were calculated at 6-31G* and are in au.

Reaction energetics for reaction 2 are listed in Table I. The zero-point energies of the reactants, transition state, and product, calculated using the 3-21G basis set, differ by less than 1 kcal mol^{-1}, and can be neglected. Both the energy of reaction and the barrier height are dependent on the basis set. The reaction energy is grossly underestimated at 3-21G (−22.23 kcal mol^{-1}) but is nearly identical at 3-21G(*) and 6-31G* (−68.37 and −68.60 kcal mol^{-1}, respectively). The barrier height is estimated as 28.31 kcal mol^{-1} at 6-31G*.

Since long bond distances and (formally) charged atoms are involved, we were also concerned with the need for diffuse functions.[8,11] We determined the energy of the transition structure at HF/6-31+G*//HF/6-31G* but, due to CPU time restrictions, we used the more symmetrical geometry of TS3 rather than TS4. The reaction energy is calculated to be −65.53 kcal mol^{-1} with a barrier of 30.32 kcal mol^{-1}, little different from the 6-31G* results.

Optimization of the TS including electron correlation is beyond our computational resources; however, based on the relatively small changes brought about by correlation in reaction 3 and the fact that TS geometries for S_N2 reactions are relatively unaffected by correlation,[11] our conclusions using the HF results should not be seriously affected by electron correlation.

Discussion

The large exothermicity of reaction 2 clearly indicates the greater ability of phosphorus to expand its octet, compared to nitrogen. The smaller reaction barrier for reaction 2 (28.3 kcal mol^{-1} at HF/6-31G*) compared to reaction 3 (30.4 kcal mol^{-1} at the same level) suggests that phosphorus acts as a stronger nucleophile towards oxygen than nitrogen, but this conclusion should be applied only for reactions yielding the oxides, since the clear preference of *P*-oxides over *N*-oxides is certainly affecting the reaction energetics.

The major difference between the transition structures for reaction 2 and reaction 3 is the angle formed by the incoming nucleophile with the N–O bond. For the identity reaction of reaction 3, the nucleophile attacks along a linear backside approach, in complete agreement with the classical S_N2 reaction mechanism. Inspection of the frontier molecular orbitals of ammonia, displayed in Figure 3, corroborate this linear arrangement. Both the HOMO and LUMO are predominantly comprised of the nitrogen p-orbital directed along the 3-fold symmetry axis, aligned for linear interaction with the *N*-oxide.

The P–O–N angle in the transition state for reaction 2 is 170.66° at 6-31G*. This transition structure is bent to maximize the interaction of the phosphine LUMO. Unlike ammonia, where the LUMO is of a_1 symmetry, the LUMO of phosphine is of *e* symmetry, the two degenerate orbitals being P–H antibonding (see Figure 3). In order to maximize the interaction of one of these degenerate LUMO's with the orbitals of the *N*-oxide, phosphine approaches at a nonlinear angle, presenting preferentially one lobe of the phosphorus p-orbital. One should keep in mind that the bent approach (C_s) is not dramatically favored over the linear attack (C_{3v}); the energy difference is only 0.04 kcal mol^{-1} at 6-31G*.

Table II. Bond Distance and $\rho(r_c)$ at 6-31G*

molecule	r(N–O)[a]	ρ(N–O)[b]	r(P–O)[a]	ρ(P–O)[b]
NH_3O	1.3765	0.3356		
PH_3O			1.4645	0.2342
TS4	1.8673	0.0083	2.1780	0.0642
TSI	1.9888	0.0612		

[a] Bond distance in angstroms. [b] Electron density at the bond critical point (e au^{-3}).

While the N–O–P angle in TS4 is not linear, the deviation from linearity is small. We therefore predict that nucleophilic attack in this reaction is restricted to near-linear backside attack, suggesting that a system having a linked nucleophile (PH_3), reacting center (O) and leaving group (NH_3) will react intermolecularly. The same is true for the analogous system having a nitrogen-based nucleophile, as typified by reaction 3.

Some information concerning the nature of the transition state can be inferred from the energy barrier, geometry and electron density distribution. In Table II we list the N–O and P–O bond distances in HN_3O, PH_3O, TS4, and TSI. The P–O and N–O distances in TS4 are 48.7% and 35.6% longer than in the oxides. Reaction 2 is very exothermic, and Hammond's postulate[12] suggests an early transition state, exactly as indicated by the bond lengths in TS4. Reaction 3 is an identity reaction and the TS must be symmetrical. Comparison of the two transition structures show the N–O bond in TSI is longer than in TS4 and the barrier height is also larger. These results further support an early TS in reaction 2.

The topological electron density method rigorously defines the ridge of maximum electron density between two bonded atoms.[13] The point along this ridge having the lowest electron density is defined as the bond critical point r_c.[14] The value of the electron density at this point, $\rho(r_c)$, has been shown to reflect the bond order[15] and can thus be used to indicate the degree of bond change during a reaction.[11] The values of ρ(P–O) and ρ(N–O) in TS4 are 27.4% and 26.3% of their respective values in the oxides. The similar degree of change in both bonds lies in contrast with the geometrical data discussed above and indicates a much more synchronous reaction. Density apparently can rearrange in advance of the molecular geometry. Finally, all the evidence consistently implies that both reaction 2 and reaction 3 proceed by a classical backside attack S_N2 reaction.

Conclusion

The identity reaction involving H_3NO and NH_3 is calculated to have a barrier of 30.39 kcal mol^{-1} at HF/6-31G*

(11) Shi, Z.; Boyd, R. J. *J. Am. Chem. Soc.* **1989**, *111*, 1575.

(12) Hammond, G. S. *J. Am. Chem. Soc.* **1955**, *77*, 334.

(13) Runtz, G. R.; Bader, R. F. W.; Messer, R. R. *Can. J. Chem.* **1977**, *55*, 3040.

(14) Bader, R. F. W.; Anderson, S. G.; Duke, A. J. *J. Am. Chem. Soc.* **1979**, *101*, 1389.

(15) (a) Bader, R. F. W.; Tang, T.-H.; Tal, Y.; Biegler-Konig, F. W. *J. Am. Chem. Soc.* **1982**, *104*, 940, 946. (b) Knop, O.; Boyd, R. J.; Choi, S. C. *J. Am. Chem. Soc.* **1988**, *110*, 7299. (c) Bachrach, S. M. *J. Comput. Chem.* **1989**, *10*, 392.

and 37.34 kcal mol^{-1} at MP2/6-31G*. The barrier for the reaction of H_3NO and PH_3 is 28.31 kcal mol^{-1} at HF/6-31G*//HF/6-31G* and increases by only 2.01 kcal mol^{-1} with the inclusion of diffuse functions.

We conclude that nucleophilic displacement at the oxygen in an *N*-oxide will proceed via an S_N2 pathway, whether the nucleophile is nitrogen or phosphorus based. Nitrogen nucleophiles will attack in a linear approach, while phosphorus nucleophiles are predicted to attack at a slightly askew angle, though not at a small enough angle to allow for intramolecular S_N2 substitution via a 5- or 6-membered ring TS. This difference can be explained in terms of the difference in the nature of the LUMOs of the nucleophiles. Finally, nucleophilic substitution at the oxygen of an *N*-oxide proceeds by a mechanism different than in reaction 1, where the proposed mechanism[5] for displacement at the oxygen of an hydroxylamine involves an addition step. Further investigations of displacement reactions at oxygen are underway and will be reported in due course.

Acknowledgment. I thank Dr. Peter Beak for suggesting the problem and providing helpful comments and the donors of the Petroleum Research Fund, administered by the American Chemical Society, for support.

Supplementary Material Available: Z-Matrices, as used in GAUSSIAN-86, and energies for all structures reported (8 pages). Ordering information is given on any current masthead page.

Kinetics of the Acetate Ion Catalyzed Ketonization of 1,3-Cyclohexadienol: Equilibrium Constants for the Enolization of 2- and 3-Cyclohexenone

Greg D. Dzingeleski, Grzegorz Blotny, and Ralph M. Pollack*

Laboratory for Chemical Dynamics, Department of Chemistry and Biochemistry, University of Maryland Baltimore County, Baltimore, Maryland 21228

Received June 30, 1989

The conjugated enol 1,3-cyclohexadienol (**2**) has been generated in aqueous solution by the acid phosphatase catalyzed hydrolysis of 1,3-cyclohexadienyl phosphate. In acetate buffers (pH 4.2–5.1), **2** ketonizes almost exclusively to the unconjugated ketone 3-cyclohexenone (**1**), rather than the conjugated ketone 2-cyclohexenone (**3**). The rate constants for acetate-catalyzed ketonization of **2** (k^{OAc} = 16.3 ± 1.5 M^{-1} s^{-1}) and for acetate ion catalyzed deuterium exchange of the C-2 hydrogen of **1** (k_{ex}^{OAc} = (9.3 ± 1.5) × 10^{-5} M^{-1} s^{-1}) were utilized, along with extrapolated literature data on the general base catalyzed isomerization of **1** → **3**, to calculate all of the microscopic rate constants for the isomerization of **1** → **3**. These rate constants provide values for the keto–enol equilibrium constants for 3-cyclohexenone (pK_E = 5.3) and 2-cyclohexenone (pK_E = 7.7).

Introduction

The properties of enols of aldehydes and ketones in both the gas phase[1] and solution phase[2] have intrigued chemists for a long time. Although enols of monofunctional aldehydes and ketones are generally unstable (both thermodynamically and kinetically) in aqueous solution and they rapidly revert back to the carbonyl compounds, Kresge,[2a] Capon,[2b] and their co-workers have developed methods to generate solutions of these enols in greater than equilibrium concentration and to investigate their rates of ketonization. This work has been instrumental in elucidating the properties of simple enols and has provided rate constants for ketonization, keto–enol equilibrium constants, and pK_a's for both enols and ketones. In a complementary study, Rappoport's group[2c] has examined the keto–enol equilibria of a variety of sterically hindered, polyaryl-substituted, stable enols.

In our laboratory,[3] we have been interested in the properties of conjugated dienols and dienolate ions as intermediates in the isomerization of β,γ-unsaturated ketones to their α,β-unsaturated isomers (eq 1), both in the absence and the presence of the enzyme steroid isomerase.[4] Although dienols have often been generated and observed,[5] it is only recently that their rates of ketonization have been determined in aqueous solution.[3,4b,6] We report here the generation of 1,3-cyclohexadienol and its rate of ketonization in acetate buffer to a mixture consisting of predominantly 3-cyclohexenone (**1**) with minor amounts of 2-cyclohexenone (**3**). These results, in combination with the rates of exchange of the 2-hydrogens of **1** and literature data on the isomerization of **1** → **3**, allow the determination of all the microscopic rate constants for the isomerization of **1** → **3** and the keto–enol equilibrium constants for both **1** ⇌ **2** and **3** ⇌ **2**. In addition, we are able to estimate the

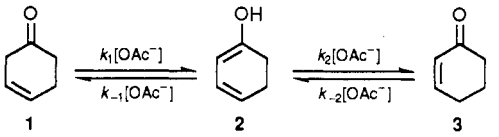

(1)

(1) Turecek, F.; Brabec, L.; Korvola, J. *J. Am. Chem. Soc.* **1988**, *110*, 7984 and references therein.

(2) For recent reviews, see: (a) Kresge, A. J. *CHEMTECH* **1986**, 250. (b) Capon, B.; Guo, B.-Z.; Kwok, F. C.; Siddhanta, A. K.; Zucco, C. *Acc. Chem. Res.* **1988**, 135. (c) Rappoport, Z.; Biali, S. *Acc. Chem. Res.* **1988**, 442.

(3) (a) Pollack, R. M.; Mack, J. P. G.; Blotny, G. *J. Am. Chem. Soc.* **1987**, *109*, 3138. (b) Pollack, R. M.; Mack, J. P. G.; Eldin, S. *J. Am. Chem. Soc.* **1987**, *109*, 5048. (c) Dzingeleski, G. D.; Bantia, S.; Blotny, G.; Pollack, R. M. *J. Org. Chem.* **1988**, *53*, 1540. (d) Pollack, R. M.; Zeng, B.; Mack, J. P. G.; Eldin, S. *J. Am. Chem. Soc.* **1989**, *111*, 6419.

(4) For reviews, see: (a) Pollack, R. M.; Bevins, C. L.; Bounds, P. L. in *The Chemistry of Functional Groups, Enones*; Patai, S., Rappoport, Z., Eds.; Wiley: Chichester, UK, 1989; p 559. (b) Capon, B. *Ibid.* p 1063.

(5) (a) Schmidt, E. A.; Hoffmann, H. M. R. *J. Am. Chem. Soc.* **1972**, *94*, 7832. (b) Noyori, R.; Inoue, H.; Katô, M. *J. Am. Chem. Soc.* **1970**, *92*, 6699. (c) Noyori, R.; Inoue, H.; Katô, M. *Bull. Chem. Soc. Jpn.* **1976**, *49*, 3673. (d) Turecek, F.; Havlas, Z. *J. Org. Chem.* **1986**, *51*, 4066.

(6) (a) Duhaime, R. M.; Weedon, A. C. *J. Am. Chem. Soc.* **1985**, *107*, 6723. (b) Duhaime, R. M.; Weedon, A. C. *J. Am. Chem. Soc.* **1987**, *109*, 2479. (c) Duhaime, R. M.; Weedon, A. C. *Can. J. Chem.* **1987**, *65*, 1867. (d) Capon, B.; Guo, B. *J. Am. Chem. Soc.* **1988**, *110*, 5144.

0022-3263/90/1955-1019$02.50/0